

Laser induced breakdown spectroscopy of pure aluminum with high temporal resolution

Yu-Tai Li,^{1,*} Tze-An Liu,¹ Chen-Wei Chen,¹ Yu-Hsien Lee,¹ and Atsushi Yabushita²

¹Center for Measurement Standards, Industrial Technology Research Institute, 321, Sec.2, Kuang Fu Rd., Hsinchu, 300, Taiwan

²Department of Electrophysics, National Chiao-Tung University, 1001 Ta Hsueh Road, Hsinchu, 300, Taiwan
*YTLi@itri.org.tw

Abstract: We report on a Laser Induced Breakdown Spectroscopy (LIBS) system with a very high temporal resolution, using femtosecond and picosecond pulse laser excitation of pure aluminum (Al). By using a 140 fs Ti:Sapphire laser in an ultrafast optical Kerr gate (OKG), we demonstrate LIBS sampling with a sub-ps time resolution (0.8 ± 0.08 ps) in a 14 ns window. The width of the gating window in this system was as narrow as 0.8 ps, owing to the inclusion of a carbon disulfide (CS₂) cell, which has a fast response and a large nonlinear coefficient. Furthermore, when using a 100 ps pulsed Nd:YAG laser and a fast photomultiplier tube (PMT) we demonstrate a LIBS system with a nanosecond time resolution (2.20 ± 0.08 ns) in a microsecond window. With this sort of temporal resolution, a non-continuous decay in the Al signal could be observed. After 50 ns decay of the first peak, the second peak at 230 ns is started to perform. Experimental results with such short temporal windows in LIBS, in both nanosecond and microsecond ranges, are important for fast temporal evolution measurements and observations of early continuum emission in materials.

©2013 Optical Society of America

OCIS codes: (300.6365) Spectroscopy, laser induced breakdown; (300.6500) Spectroscopy, time-resolved; (320.7110) Ultrafast nonlinear optics.

References and links

1. J. D. Winefordner, I. B. Gornushkin, D. Pappas, O. I. Matveev, and B. W. Smith, "Novel uses of lasers in atomic spectroscopy," *J. Anal. At. Spectrom.* **15**(9), 1161–1189 (2000).
2. E. H. Evans, J. A. Day, C. D. Palmer, W. J. Price, C. M. M. Smith, and J. F. Tyson, "Atomic spectrometry update. Advances in atomic emission, absorption and fluorescence spectrometry, and related techniques," *J. Anal. At. Spectrom.* **20**(6), 562–590 (2005).
3. B. E. Naes, S. Umpierrez, S. Ryland, C. Barnett, and J. R. Almirall, "A comparison of laser ablation inductively coupled plasma mass spectrometry, micro X-ray fluorescence spectroscopy, and laser induced breakdown spectroscopy for the discrimination of automotive glass," *Spectrochim. Acta, B At. Spectrosc.* **63**(10), 1145–1150 (2008).
4. M. R. Leahy-Hoppa, J. Miragliotta, R. Oslander, J. Burnett, Y. Dikmelik, C. McEnnis, and J. B. Spicer, "Ultrafast Laser-Based Spectroscopy and Sensing: Applications in LIBS, CARS, and THz Spectroscopy," *Sensors (Basel)* **10**(5), 4342–4372 (2010).
5. F. J. Fortes, J. Cuñat, L. M. Cabalín, and J. J. Laserna, "In situ analytical assessment and chemical imaging of historical buildings using a man-portable laser system," *Appl. Spectrosc.* **61**(5), 558–564 (2007).
6. J. Wu, Y. Zou, X. Zhan, S. Chen, G. Lu, and F. Lai, "Survey of heavy metal pollution in four chinese crude drugs and their cultivated soils," *Bull. Environ. Contam. Toxicol.* **81**(6), 571–573 (2008).
7. D. W. Hahn and N. Omenetto, "Laser-Induced Breakdown Spectroscopy (LIBS), Part I: Review of Basic Diagnostics and Plasma-Particle Interactions: Still-Challenging Issues Within the Analytical Plasma Community," *Appl. Spectrosc.* **64**(12), 335–366 (2010).
8. C. Hermann, J. S. Bruneau, and M. Sentis, "Spectroscopic analysis of femtosecond laser-induced gas breakdown," *Thin Solid Films* **453–454**, 377–382 (2004).
9. C. Aragón and J. Aguilera, "Characterization of laser induced plasmas by optical emission spectroscopy: A review of experiments and methods," *Spectrochim. Acta, Part B* **63**(9), 893–916 (2008).
10. Y. Dikmelik, C. McEnnis, and J. B. Spicer, "Femtosecond and nanosecond laser-induced breakdown spectroscopy of trinitrotoluene," *Opt. Express* **16**(8), 5332–5337 (2008).
11. E. L. Gurevich and R. Hergenröder, "Femtosecond laser-induced breakdown spectroscopy: physics, applications, and perspectives," *Appl. Spectrosc.* **61**(10), 233–242 (2007).

12. P. Matousek, M. Towrie, A. Stanley, and A. W. Parker, "Efficient rejection of fluorescence from raman spectra using picosecond Kerr gating," *Appl. Spectrosc.* **53**(Spec.), 1485–1489 (1999).
 13. O. Barthélemy, J. Margot, S. Laville, F. Vidal, M. Chaker, B. Le Drogoff, T. W. Johnston, and M. Sabsabi, "Investigation of the state of local thermodynamic equilibrium of a laser-produced aluminum plasma," *Appl. Spectrosc.* **59**(4), 529–536 (2005).
 14. J. Hein, M. Helbig, and S. Rentsch, "Measurements of a nonlinear refractive index with a single laser pulse," *Appl. Opt.* **36**(6), 1173–1176 (1997).
 15. K. L. Eland, D. N. Stratis, D. M. Gold, S. R. Goode, and S. M. Angel, "Energy dependence of emission intensity and temperature in a LIBS plasma using femtosecond excitation," *Appl. Spectrosc.* **55**(3), 286–291 (2001).
 16. B. Le Drogoff, J. Margot, M. Chaker, M. Sabsabi, O. Barthélemy, T. W. Johnston, S. Laville, F. Vidal, and Y. Von Kaenel, "Temporal characterization of femtosecond laser pulses induced plasma for spectrochemical analysis of aluminum alloys," *Spectrochim. Acta, B At. Spectrosc.* **56**(6), 987–1002 (2001).
 17. V. I. Babushok, F. C. DeLucia, Jr., P. J. Dagdigian, J. L. Gottfried, C. A. Munson, M. J. Nusca, and A. W. Miziolek, "Kinetic modeling study of the laser-induced plasma plume of cyclotrimethylenetrinitramine (RDX)," *Spectrochim. Acta, B At. Spectrosc.* **62**(12), 1321–1328 (2007).
-

1. Introduction

Laser ablation is produced by focusing pulsed laser beams onto matter, which results in a plasma [1]. Spectral analysis of the light emitted in an ablation process provides information about the atomic composition of the sample via the spectral signatures of particular atoms, and is known as laser-induced breakdown spectroscopy (LIBS) or laser-induced plasma spectroscopy (LIPS). This quick and convenient technique has been widely used in recent years and is now considered standard analysis [2–4]. In LIBS, a laser-produced plasma may be generated from any solid, liquid or gas material without any sample preparation requirements. Thus, armed with only a laser and spectrometer, the atomic composition of matter can be determined by simply focusing the laser beam onto a sample [5]. And, since measuring times are as short as a few seconds, LIBS is considered to be a useful on-line examination technique in various industrial applications, as well as in the fields of medicine, and security [6].

Recently, some attention has been focused on the basic diagnostics aspects and plasma-particle interactions in LIBS, because the quantitative capabilities of the technique may be considered its Achilles' heel. This is a result of the complex nature of the laser-sample interaction processes, which depend on not only the material properties of a sample but also on the laser characteristics [7]. Because of the fast temporal evolution of the characteristic parameters in LIBS, there is a strong interest in improving the time resolution of measurements. For example, to measure the time evolution of spectral line emission in LIBS using nanosecond laser pulses, a time resolution on the order of 100 ns is generally considered to be adequate for windows on the time scale of microsecond. Other experimental conditions can involve faster spectral evolution ($\cong 100$ ns), where shorter temporal windows are then called for [8]. There, the necessary resolution can be achieved with fs-pulse laser excitation and fast ICCD detection [9]. Short fs-pulse laser based LIBS provides other advantages over ns-pulse laser excitation, such as improvements in material removal rates and analytic capabilities for molecular species [10]. These advantages arise because shorter laser pulses are associated with less transient changes in the thermodynamic states of materials. As a consequence, many new techniques have recently been proposed to perform spectral analysis in femtosecond LIBS experiments with microsecond gating times [11].

In this paper, we first present an OKG-based ps-gated window that provides a high temporal resolution in femtosecond LIBS experiments. The OKG is opened by passing an intense pump beam through a nonlinear gating medium between two crossed polarizers, which produce a polarization rotation of a probe beam, thus allowing it to pass. Similar effect has been applied for rejection of fluorescence from Raman spectra, in which a nonlinear and fast relaxation time medium of CS₂ is adopted [12]. In this paper, we report on a LIBS system which uses an OKG to reduce the gating time of the diagnostic. We used a Ti:sapphire laser with regenerative amplifier to excite CS₂ in a liquid cell to gate the signals, and estimated the gating efficiency and the full width half maximum (FWHM) of the resultant time window. A pure Al sample was used to demonstrate the quality of measurement of the plasma spectrum. The Al spectrum is also gated on a nanosecond timescale, in order to simulate the plasma

evolution. The result shows that we achieve a picosecond time-resolution within a 20 ns window, limited only by a time delay caused by distance. In the end, we performed a quantitative analysis of early continuum emission.

In a second experiment, we employed a 100-ps high energy Nd:YAG laser as a pump beam together with a fast PMT as a detector in order to obtain a LIBS signal quickly over a longer time window ($\sim 2 \mu\text{s}$). Compared with femtosecond pulse excitation, picosecond laser pulses generate similar electron density, excitation temperatures and spatial distributions in LIBS plasma, while achieving higher excitation pulse intensity [13]. When the LIBS signal is detected directly with a fast PMT, we achieved a nanosecond time resolution within a microsecond time window.

2. Experimental set-up

2.1 Set-up of the LIBS system with OKG

Figure 1 shows a schematic of the LIBS system based on OKG. A Ti: sapphire laser with regenerative amplifier was used as the light source. The center wavelength, pulse width, repetition rate and pulse energy of the laser are 800 nm, 140 fs, 1 kHz and 0.1mJ, respectively. A lens with 5 cm focal length focused the laser onto a 5 mm thick commercial Al plate (1050, nominally 99.5 mass% Al) to generate plasma radiation. The Al sample was rotated at a constant speed to avoid the accumulation of damage on the sample. Plasma light emission from the sample was collected using a fiber optic spectrometer (Ocean Optics, USB2000, resolution 2.5 nm) whose tip was positioned close to the sample surface, and the observed spectrum is shown in Fig. 2. One can see several peaks in the spectral range from 250 nm to 450 nm, with the highest peak at around 396 nm.

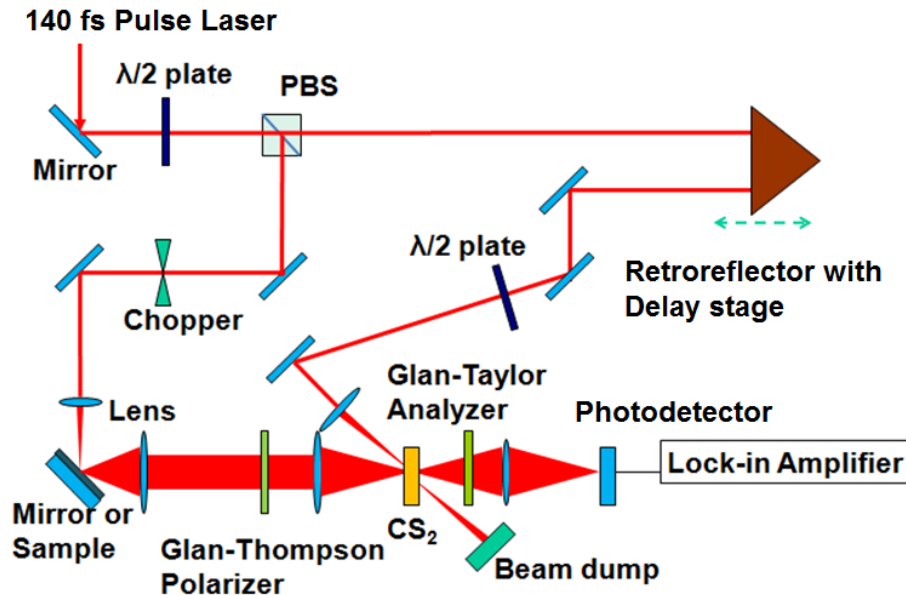


Fig. 1. Schematic diagram of LIBS based on OKG and a femtosecond laser. The mirror in the left corner was used while measure the instrument response function (IRF) of the system directly. Sample (Al plate) was used to replace the mirror in measurement of LIBS of Al.

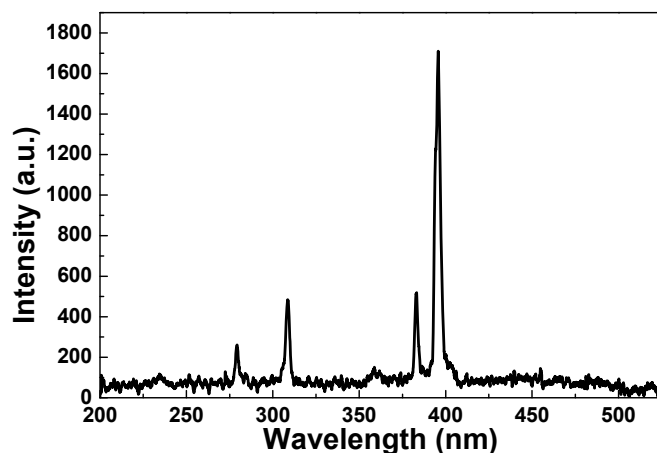


Fig. 2. Emitted Al spectrum measured by a fiber optic spectrometer.

The intensity ratio between the gating beam and probe beam was adjusted via a half-wave ($\lambda/2$) plate and a polarization beam splitter (PBS). Both beams were focused onto a CS₂ liquid cell via two lenses, each with 15 cm focal length. In the path of the gate pulse, a retroreflector, mounted on a motion-controlled linear stage, was inserted to serve as an optical delay line, and a $\lambda/2$ plate oriented the gate polarization at 45° with respect to the probe polarization. Using a chopper in the probe beam path, we modulated the probe signal at 248 Hz for lock-in detection of the probe signal. The noise in the probe beam, which should be vertically polarized, was removed by inserting a Glan-Thompson polarizer in front of the CS₂ cell. The induced change in the refractive index of CS₂ depends on the gating beam intensity according to the Kerr effect, i.e. n_2I , where $n_2 = 3.1 \times 10^{-18} \text{ m}^2/\text{W}$ [14]. Upon excitation of CS₂ by the gating beam, the refractive index of CS₂ was changed, causing a rotation in the polarization of the probe beam.

After the probe beam passes through the CS₂ cell, a Glan-Taylor polarizer (analyzer) was inserted to transmit only light with horizontal polarization, which removed that probe beam component which did not interact with the gating beam. The CS₂ performed as a $\lambda/2$ plate when the intensity of the gating beam increased to some optimum value [12]. At that point, the probe beam is transmitted through the Glan-Taylor analyzer and impinges onto a photo detector. Finally, the detected signal is processed to reject any ambient light noise by way of a lock-in amplifier.

2.2 Set-up of the LIBS system with fast PMT

As shown in Fig. 3, for quick and easy measurements of the time response of the Al plasma in the time period of interest (up to 2000 ns), we excited our sample with a higher energy Nd:YAG laser pulse (10 mJ, 1064 nm, 10 Hz, 100 ps), and measured the resultant signal directly from a 500-MHz oscilloscope with a fast PMT (H957-08, HAMAMATSU, 2.2 ns response time) at each probe wavelength. Each wavelength was scanned with a spectrometer (iHR320, HORIBA, Jobin Yvon, resolution 0.3 nm) containing a grating with 300 grooves per mm.

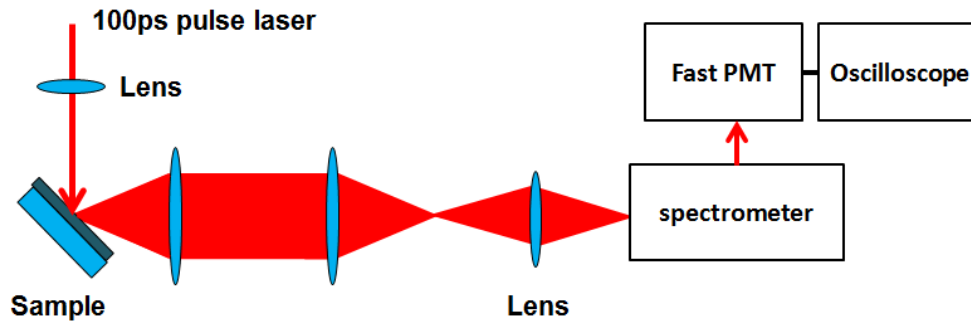


Fig. 3. LIBS system using a fast PMT and picosecond laser pulses.

3. Results and discussion

3.1 Instrument response function

Figure 4 shows the instrument response function (IRF) of the LIBS system based on OKG, which was obtained by putting a mirror in place of the Al sample. At first, the focus lens before mirror was not used and incident power was reduced to avoid the damage of the mirror. The signal to noise ratio of the observed signal was estimated to be over 1000. The satellite peak seen in front of the main peak can be attributed to the coherent coupling of the pump beam, which is scattered by a transient grating that is induced by pump and probe beams in the CS₂ cell.

Afterwards, we replaced the reflecting mirror shown in the lower left corner of Fig. 1 with the Al sample and increased laser power to 100 mW. With a focused spot diameter of $\sim 20\mu\text{m}$, the energy density of 10 J/cm^2 (power density: 60 TW/cm^2) could be obtained. The inset of Fig. 4 shows the cross-correlation signal between the gate pulse and the light scattered from an Al target with a FWHM of $\sim 1.1\text{ ps}$, which is of longer duration than that of the signal reflected from a mirror (0.8 ps). This might be attributed to variations in the incident angle that results in scattering phenomena caused by the rougher surface of Al target compared with the mirror.

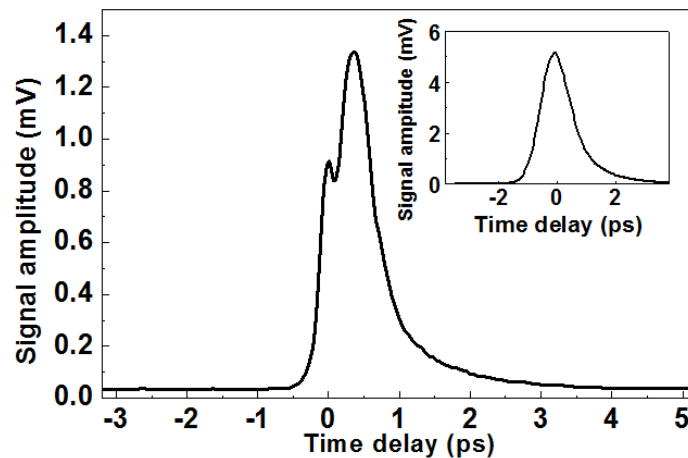


Fig. 4. Measured temporal response waveform of Ti: sapphire laser when laser was reflected from a mirror. The inset shows the waveform when the laser beam was reflected by Al sample.

3.2 LIBS of Al plasma

In the measurement of LIBS of Al plasma, the same Al sample was used. By inserting a bandpass filter (center wavelength: 396 nm, bandwidth: 16 nm) between the Al sample and CS₂ cell in Fig. 1, we optimized the alignment of the detection system. Then, the Kerr gated Al plasma spectrum was obtained by replacing our detector with an optical spectrometer (iHR320, HORIBA, Jobin Yvon) combined with a built-in UV-VIS PMT (DPM-HV, HORIBA, Jobin Yvon). By moving the position of the retroreflector, we could observe the signal for setting the gating window to run from 2.5 ns to 14 ns. Figure 5 shows the spectrum intensity recorded by the spectrometer while the delay stage was fixed at positions with time delay 2.5 ns and 14 ns separately. Each measurement was averaged in 20 seconds with 20000 pulses while automatically scanned by the spectrometer from 385 nm to 410 nm with an interval of 0.25 nm.

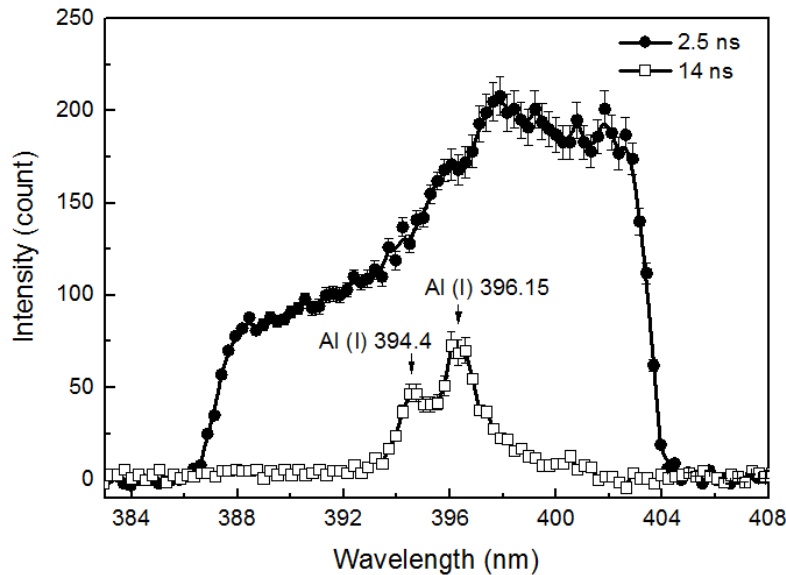


Fig. 5. Kerr gated Al Plasma at delays of 2.5 ns and 14 ns. The error bars near peaks show the standard deviations. Two Al neutral emission lines were also labeled at 394.4 nm and 396.15 nm.

In this window, the plasma at early times is a near continuum emission, while two narrow peaks near two Al neutral lines (394.4 nm and 396.15 nm) emerge at later time, in agreement with femtosecond LIBS theory [15,16]. In addition, in contrast with previous femtosecond LIBS based Al emission results with similar pulse energy density $\sim 20 \text{ J/cm}^2$ [16], we were able to resolve the intensity evolution gap in the early continuum emission (0 \sim 0.4 μs) with a picosecond time resolution (0.8ps) by using the OKG. The Al plasma spectrum is quite broad at 14 ns, and is expected to narrow in the time after 10 ns.

3.3 Time-resolved LIBS with fast PMT

In order to get LIBS signal over a longer time ($\sim 2 \mu\text{s}$), we employed a 100-ps high energy Nd:YAG laser as a pump beam together with a spectrometer and a fast PMT as shown in Fig. 3. In the set-up, higher pulse energy density $\sim 800 \text{ J/cm}^2$ (power density: 10 TW/cm^2) with the same focus spot size could be estimated. The LIBS intensity change versus with time at each wavelength was directly measured through an oscilloscope while wavelength was scanned at a 5 nm interval manually with the spectrometer. Figure 6 shows the temporal evolution of the Al plasma spectrum observed from 0 to 2000 ns. At every wavelength, 10 pulses were needed for each scan within 1 second in time domain from 0 to 2000 ns. The time resolution of the

time-resolved LIBS spectrum with a fast PMT obtained was ~ 2 ns, much better than general time-resolved LIBS data one gets with a gated CCD spectrometer (>10 ns) [15,16]. Our results illustrate the narrowing of the Al plasma spectrum in its temporal evolution after 10 ns.

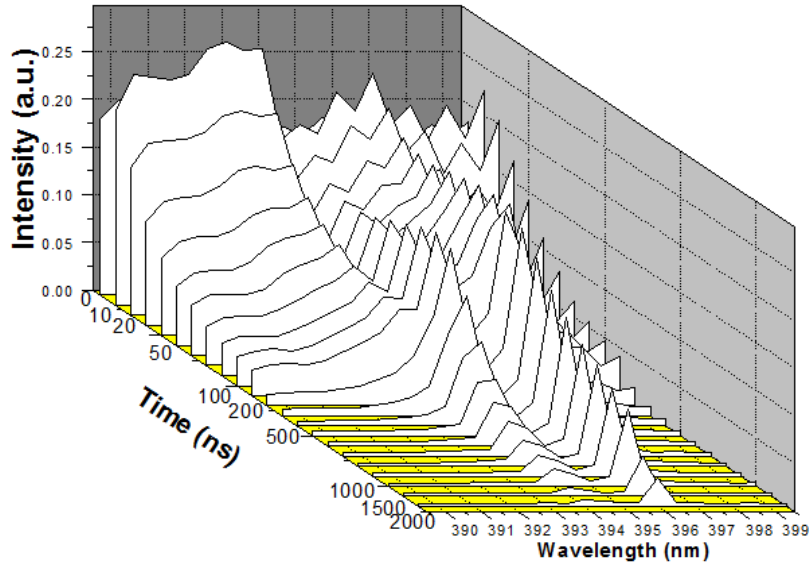


Fig. 6. 3D view of the temporal evolution of the Al plasma for experiments using a 10 mJ 1064 nm Nd: YAG laser and fast PMT (no OKG).

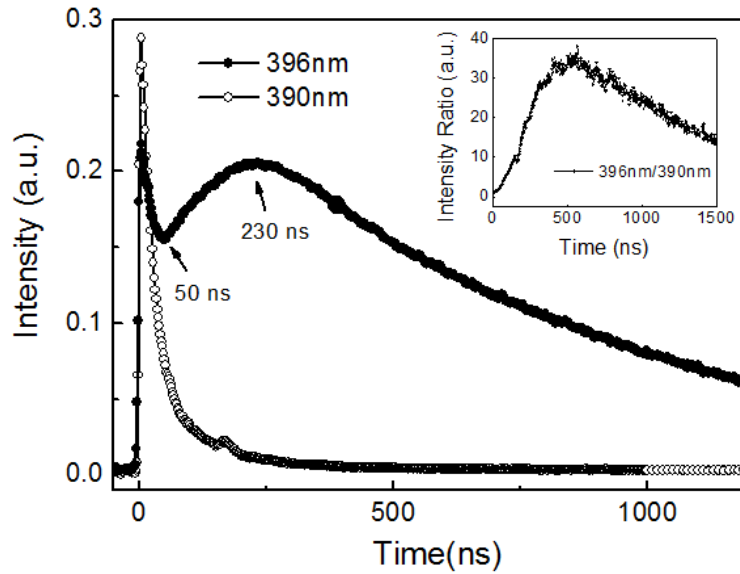


Fig. 7. Temporal evolution of Al plasma emission at wavelengths of 396 nm and 390 nm as background.(no OKG). The inset shows the intensity ratio of these two wavelengths.

In Fig. 7, we compared the signal in Fig. 6 probed at the Al emission wavelength (396 nm, closer to 396.15 nm) with probed signal at the background (390 nm). The intensities of both wavelengths exhibit a similar decay in the first 50 ns. After that, between 50 and 230 ns, an

increase in the Al emission could be observed, while the background wavelengths continue to decay. Finally, a slower decay for the Al emission signal could be observed after 230ns. Such transiently enhanced signals have also been observed in Pb atomic emission in experiments with LIBS with 10 ns time resolution [5]. Finally, as the inset of Fig. 7 shows, the S/N ratio (intensity ratio of 396.5/395.5 nm) increases 35-fold over the time from $t = 0$ to 500 ns. Thus, the line emission of Al relative to the initial broad background could be enhanced by choosing gate delay quickly through this method.

4. Conclusion

In conclusion, we demonstrated very short temporal windows on both the nanosecond and microsecond scales for LIBS spectra from pure Al. An OKG based ultrafast LIBS system with a CS₂ Cell provides sub-ps time resolution in the evolution of the early continuum within a 14 ns window.

For times after 10 ns, additional spectral narrowing was observed by using high energy picosecond laser pulses, a fast PMT, and a spectrometer. The time resolution (~2.5ns) achieved in this system is superior to what is obtained by general time-resolved LIBS systems that use gated CCD spectrometers as detectors (>10 ns). Instruments with superior temporal resolution are desirable for the observation of fast evolution phenomena, which is particularly relevant for complex molecular species in LIBS samples, such as in the area of explosives detection [17]. In addition, our method also provides a way to understand source of LIBS including plasma-particle interactions happened in a very short time.